Combined acceleration of electrons by whistler-mode and compressional ULF turbulences near the geosynchronous orbit

Liuyuan Li,[1] Jinbin Cao, and Guocheng Zhou

Center for Space Science and Applied Research, Chinese Academy of Sciences, Beijing, China

Received 14 June 2004; revised 19 November 2004; accepted 2 December 2004; published 4 March 2005.

[1] In the quasi-linear approximation, we study electron acceleration process generated by whistler-mode and compressional ULF (fast mode waves) turbulences near the Earth's synchronous orbit. The results show that the whistler-mode turbulence ($0.1f_{ce} \leq f \leq 0.75f_{ce}$) can accelerate substorm injection electrons with several hundreds of keV through wave-particle gyroresonant interaction and hence may play an important role in the electron acceleration during substorms. The compressional ULF turbulence (2–15 mHz) can accelerate both lower-energy background electrons (<30 keV) and substorm injection electrons (~30–300 keV) through the transit-time damping mechanism. So the compressional ULF turbulence acceleration mechanism is important during both substorms and quiet times. The compressional ULF turbulence accelerates substorm injection electrons more effectively than whistler-mode turbulence. The combined electron acceleration by whistler-mode and ULF turbulences is most effective and can cause the number density of the relativistic electrons increase largely within about 8 hours. Substorms can offer both substorm injection electrons and strong turbulences, and therefore large flux enhancement events of relativistic electrons (≥1 MeV) always occur during substorm time. For magnetic storms that are composed of a series of substorms, extremely large flux enhancement events of the relativistic electrons can thus occur.

Citation: Li, L., J. Cao, and G. Zhou (2005), Combined acceleration of electrons by whistler-mode and compressional ULF turbulences near the geosynchronous orbit, *J. Geophys. Res.*, *110*, A03203, doi:10.1029/2004JA010628.

1. Introduction

[2] During the time of high-speed solar wind with a southward component of the IMF, geomagnetic storms/substorms and the flux enhancements of relativistic electrons (≥1 MeV) are frequently observed in the outer radiation belt ($3 \leq L \leq 7$) [*Baker et al.*, 1998; *Blake et al.*, 1997; *Li et al.*, 1999; *Reeves*, 1998; *Zhou et al.*, 2001; *Selesnick and Blake*, 1998; *Iles et al.*, 2002; *Cao et al.*, 2002]. Typically, fluxes of relativistic electrons decrease during the main phase of a magnetic storm and then increase to exceed the prestorm level by a factor of 10 or higher during the recovery phase. The relativistic electron enhancement occurs first from the electrons with the pitch angle of 90°, and then the pitch angle distribution became more isotropic than that of the prestorm distribution [*Nakamura et al.*, 2002; *Miyoshi et al.*, 2003]. Since relativistic electrons have enough energy to penetrate the outer skin of spacecraft and cause internal charging, they can cause spacecraft anomalies or destroy a spacecraft completely [*Wrenn and Smith*, 1996].

[3] However, not all storms are associated with relativistic electron flux enhancements. *Reeves et al.* [2003] analyzed the response of relativistic electrons for 276 moderate and intense geomagnetic storms spanning the 11 years from 1989 through to 2000 and found that about half of all storms increased the fluxes of relativistic electrons, one quarter decreased the fluxes, and one quarter produced little or no change in the fluxes. They suggested that high-speed solar wind streams increase the probability of a large flux increase. *Meredith et al.* [2002], by analyzing plasma wave and particle data from the CREES satellite, suggested that prolonged substorm ($AE > 100$ nT) activities in the recovery phase of a storm are required for relativistic electron flux enhancements. In fact, fast solar wind streams southward disturbances of the IMF can lead to substorm activities and enhance waves [*Baker et al.*, 1998; *Mathie and Mann*, 2000; *Russell*, 2000; *O'Brien et al.*, 2003], such as whistler-mode waves and compressional ULF (ultra low frequency) waves and so on in the magnetosphere. The substorm activities produce hot electrons with energy up to a few hundred keV due to enhanced storm time convection electric fields or other mechanism. It is clear that there are very close relationships among the substorm injection electron population, waves, and relativistic electron flux enhancements.

[4] Recent studies provide strong evidences for the local stochastic electron acceleration by wave-particle inter-

[1] Also at Graduate School of the Chinese Academy of Sciences, Beijing, China.

0148-0227/05/2004JA010628

actions involving whistler-mode chorus and the electrons can be accelerated to relativistic energy range [*Horne et al.*, 2003; *Summers and Ma*, 2000a; *Meredith et al.*, 2003; *Miyoshi et al.*, 2003; *Li et al.*, 2004]. Some other studies show that the drift resonance between electrons and toroidal mode ULF waves can transport electrons radially inward and make them energized [*Elkington et al.*, 1999, *Hudson et al.*, 2000, 2001; *Nakamura et al.*, 2002]. Finally, if electron pitch angle scattering is sufficiently rapid to maintain an isotropic distribution function, the compressional magnetic field component (along background magnetic field) of compressional ULF (fast mode waves) can also resonate with these electrons and energize them via transit time damping [*Summers and Ma*, 2000b]. Undoubtedly, electron accelerations by different waves are most important causes of the enhancements of relativistic electron flux in the outer radiation belt, but most previous studies focused on the electron acceleration by only one kind of waves.

[5] In fact, the relativistic electron flux enhancements are different when different waves exist in the magnetosphere. Statistic results show that storms with neither strong ULF waves nor whistler-mode waves have the lowest flux of MeV electrons; storms with only ULF waves or whistler-mode waves have a somewhat higher flux of MeV electrons; and storms with both strong ULF waves and whistler-mode waves have the highest flux of poststorm MeV electrons at $L \sim 4.5$ [*O'Brien et al.*, 2003]. Furthermore, ULF waves and whistler-mode waves interact together with electrons in many regions. For example, Polar/HIST, HEO, and LANL satellites measured a series of global relativistic electron flux enhancements that are associated with substorm activities in January 1997 [*Baker et al.*, 1998]; a rapid flux enhancement observed by LANL satellite took place within about 12 hours after the midday of 10 January. At the same time, some low-frequency waves with fluctuating magnetic field amplitude of 50 nT were measured at various CANOPUS ground stations [*Baker et al.*, 1998]. Moreover, compressional waves with strongest signals at 1–15 mHz were observed by GEOTAIL at 2100–2400 (UT) on 10 January 1997, and these fast mode waves have much broader power spectra than the narrow-banded field-line resonances with a toroidal mode simultaneously observed by POLAR at $L = 10.2$–6.6 [*Laakso et al.*, 1998]. In addition, VLF chorus with fluctuating intensity up to ~100 pT is observed by POLAR during 10 January 1997 [*Lauben et al.*, 1998]. We also investigated the VLF/ELF wave data from GEOTAIL and found that VLF/ELF wave activities were enhanced markedly on that day. GEOTAIL satellite went through geosynchronous altitude ($L \sim 6.6$) four times at about 0100 UT, 0800 UT, 1000 UT and 2200 UT, respectively. In this case, electrons, whistler-mode, and compressional ULF waves may possibly exist in the same region at the same time. Thus electrons will probably be accelerated jointly by whistler-mode waves and ULF waves.

[6] In this paper, we focus on the combined acceleration process of trapped electrons by whistler-mode and compressional ULF turbulences near the Earth's geosynchronous orbit. The initial trapped electrons consist of background hot electrons (<30 keV) and substorm injection electrons (~30–300 keV). It is assumed that the adiabatic acceleration due to radial diffusion or transport is weaker and can be ignored for strong pitch scattering of electrons caused by VLF/ELF waves.

2. Physical Model

2.1. Initial Momentum Distribution Function of Seed Electrons

[7] Since we mainly focus on the initial trapped electron accelerations, we assume that during the substorm course, the electrons near the geosynchronous orbit mainly consist of two components: substorm injection electrons and background hot electrons. Therefore the initial normalized distribution function of electrons can be given by

$$f(p) = \frac{(1-\varepsilon)}{\pi^{3/2}\Delta_b^3}\exp\left(-\frac{p^2}{\Delta_b^2}\right) + \varepsilon C \exp\left[-\frac{(p-p_0)^2}{\Delta_s^2}\right], \quad (1)$$

where Δ_s and Δ_b are the normalized thermal spreads of momentum of substorm injection electrons and background electrons, respectively, p_0 is the central momentum corresponding to the central energy of substorm injection electrons, $\varepsilon = n_s/n_b$ is the density ratio, n_s is the number density of substorm injection electrons, $n(=n_s + n_b)$ is the number density of all electrons, and n_b is the number density of background hot electrons. The density ratio ε is related to the substorm index (*AE*), and a larger ε corresponds to a larger substorm and more injected electrons. Since the substantially different substorm activity levels changed very much the intensities of low-to-moderate energy electrons at geosynchronous orbit [*Baker et al.*, 1998], p_0 may be different for different substorms too. The momentum and the thermal spreads of momentum are normalized by $m_e c$, where m_e is the rest mass of an electron, v is the electron velocity, and c is the speed of light. The momentum distribution function is normalized by $n/(m_e c)^3$. The quantity C is a constant and can be calculated from the equation $\int_0^\infty f(p)4\pi p^2 dp = 1$.

2.2. Whistler-Mode Turbulence in the Magnetosphere

[8] Whistler-mode waves are observed mainly outside the plasmapause in the frequency range $0.1 \sim 1.0\, f_{ce}$ (where f_{ce} is the electron cyclotron frequency) and can be excited by cyclotron resonance with isotropic 10–100 keV electrons over a broad range of local times (0000–1500 MLT) [*Summers et al.*, 2004], the amplitude of whistler-mode waves also depends on their locations and substorm activities. Usually, equatorial lower-band chorus in the region $3 \le L \le 7$ during active times ($AE > 300$ nT) has an amplitude $\delta B_W = 10$–100 pT [*Lauben et al.*, 1998; *Meredith et al.*, 2001].

[9] The whistler-mode wave frequency, ω, is between the proton and electron cyclotron frequencies. The dispersion relation of parallel propagation whistler-mode waves can be expressed approximately by

$$\omega = k^2/G, \quad (2)$$

where $k = k_{\|}$ is the parallel wave number, $G \equiv \omega_{pe}^2/\Omega_e^2$, ω_{pe} is the electron plasma frequency, and Ω_e is the electron cyclotron frequency. The frequency and wave number are normalized by Ω_e and Ω_e/c, respectively.

[10] Generally, the power spectral density of whistler-mode turbulence magnetic field is a Gaussion frequency distribution [*Tsurutani and Smith*, 1977; *Horne et al.*, 2003; *Summers et al.*, 2004]. $B^2(\omega)$ is normalized by Ω_e/B_0^2 and given by

$$B^2(\omega) = \begin{cases} A \exp -\left(\frac{\omega - \omega_m}{\delta\omega}\right)^2, \omega_{lc} \le \omega \le \omega_{uc} \\ 0, else\, \omega \end{cases} \quad (3)$$

where

$$A = \frac{R_W}{\delta\omega} \frac{2}{\sqrt{\pi}} \left[erf\left(\frac{\omega_m - \omega_{lc}}{\delta\omega}\right) + erf\left(\frac{\omega_{uc} - \omega_m}{\delta\omega}\right)\right]^{-1},$$

and ω_{lc}, ω_{uc}, ω_m, and $\delta\omega$ are the lowest frequency, the upper frequency, the frequency of maximum wave power, and the bandwidth. All of the frequencies are normalized by Ω_e. $R_W = (\Delta B_W/B_0)^2$, where ΔB_W is the average amplitude of whistler-mode wave magnetic field and B_0 is equatorial ambient magnetic field.

[11] The interaction between the parallel propagation whistler waves and electrons occurs through the first-order cyclotron resonance (harmonic number $m = 1$). The relativistic gyroresonant condition is given by

$$\omega = k\beta\mu + \frac{1}{\gamma}, \quad (4)$$

where $\beta = v/c$ is the normalized velocity and μ is the cosine of the electron pitch angle, $\gamma = (1 + p^2)^{1/2}$ is the Lorentz factor, and p is the normalized momentum.

2.3. Compressional ULF Turbulence in the Magnetosphere

[12] Compressional ULF turbulence intensity in the magnetosphere is larger in the case of high-speed solar wind than that in the case of low-speed solar wind. The compressional ULF turbulence may be produced in wider L range ($L \sim 3$–10) [*Higuchi and Kokubun*, 1988; *Anderson et al.*, 1990; *Zhu and Kivelson*, 1991]. The normalized dispersion relation of the compressional waves in the frequency range $\omega \ll \Omega_i$ can be written as

$$\omega = k\beta_A, \quad (5)$$

where k is the wave number of the oblique propagation mode, $\beta_A = v_A/c$, and v_A is the Alfvén speed.

[13] The power law spectrum of the compressional ULF turbulence can be expressed as the Kolmogorov type approximately [*Zhu and Kivelson*, 1991; *Schlickeiser et al.,* 1998; *Posch et al.*, 2003], and the spectral energy density $W(k)$ is assumed to take the form [*Summers and Ma*, 2000b]

$$W(k) \propto k^{-q}, k < k_{\min}, \quad (6)$$

where q (>1) is the spectral index and $k_{\min}$ is some minimum wave number.

[14] For the compressional ULF turbulences, the resonance with harmonic number $m = 0$ between the compression component of the ULF wave field and electrons (i.e., the effect of transit-time damping) can occur [*Summers and Ma*, 2000b]. The resonance condition is given by

$$\omega = k\xi\beta\mu, \quad (7)$$

where $\xi = \cos\psi$, and ψ is the propagation angle of the compressional ULF waves. We can get $\beta > \beta_A$ from equations (5) and (7), which shows that the resonance is only possible for electrons with speeds exceeding the Alfvén speed.

2.4. Momentum Diffusion Equation

[15] In the quasi-linear approximation, the temporal evolution of the momentum distribution function of electrons is controlled by the Fokker-Planck equation. Since the pitch angle scattering timescale is much shorter than the momentum diffusion timescale [*Horne et al.*, 2003], the momentum distribution of electrons can be assumed to be isotropic in the momentum diffusion process. It is assumed that sinks and sources of electrons and the spatial variation of the distribution function can be neglected in the momentum diffusion process. Then we can readily obtain a normalized momentum diffusion equation by integrating the diffusion equation over the pitch angle [*Steinacker and Miller*, 1992; *Schlickeiser and Miller*, 1998; *Summers and Ma*, 2000a, 2000b]:

$$\frac{\partial f}{\partial t} = \frac{1}{p^2}\frac{\partial}{\partial p}\left[p^2 D(p)\frac{\partial f}{\partial p}\right]. \quad (8)$$

[16] Since whistler-mode and compressional ULF waves are located in different frequency ranges, their contributions to the electron momentum diffusion can be regarded approximately as independent. Therefore the combined momentum diffusion coefficient can be written as the sum of two coefficients:

$$D(p) = D_W(p) + D_U(p), \quad (9)$$

where

$$D_W(p) = \frac{1}{2}\int_{-1}^{1}\left(D_{pp} - \frac{D_{\mu p}^2}{D_{\mu\mu}}\right)d\mu,$$

$$D_{pp}(\mu, p) = \left(1 - \mu^2\right)I_2, D_{\mu p}(\mu, p) = \frac{(1-\mu^2)}{p}\left(\frac{p}{\gamma}I_1 - \mu I_2\right),$$

$$D_{\mu\mu}(\mu, p) = \frac{(1-\mu^2)}{p^2}\left(\frac{p^2}{\gamma^2}I_0 - 2\mu\frac{p}{\gamma}I_1 + \mu^2 I_2\right),$$

$$I_l(\mu, p) = \pi A \sum_r \exp\left[-\left(\frac{\omega_r - \omega_m}{\delta\omega}\right)^2\right]\left(\frac{k_r}{G}\right)^l \left|\mu\frac{p}{\gamma} - \frac{2k_r}{G}\right|^{-1},$$

$$l = 0, 1, 2$$

$$k_r = k_\pm = \frac{G}{2\gamma}\left[\mu p \pm \sqrt{(\mu p)^2 + \frac{4\gamma}{G}}\right];$$

and

$$D_U(p) = \frac{\pi(1-q)}{4} R_U \gamma p^{q-1} (k_{\min})^{q-1} \beta_A^2 I(x, \beta_A, k_{\min}),$$

$$I(x, \beta_A, k_{\min}) = \begin{cases} c_1(q) \log(1/x), 1 < q \le 2, \\ c_2(q) p^{(2-q)} k_{\min}^{(2-q)} \log(1/x), q > 2, \end{cases}$$

$$c_1(q) = 2^{(1-q)} \frac{q}{4-q^2} \frac{\Gamma(q)\Gamma(2-q/2)}{\Gamma^3(1+q/2)},$$

$$c_2(q) = \frac{2q^2-3q+4}{4q(2q-3)}, x = \beta_A/\beta = \gamma\beta_A/p, R_U = \left(\frac{\Delta B_U}{B_0}\right)^2.$$

$D_W(p)$ is the momentum diffusion coefficient of whistler-mode turbulence, k_r is resonant wave numbers for resonance between whistler-mode waves and electrons with different energies, the k_+ is for whistler-mode waves traveling parallel to ambient magnetic field, and the k_- is for the whistler-mode waves traveling antiparallel. $D_U(p)$ is the momentum diffusion coefficient of compressional ULF waves. ΔB_U is the average amplitude of compressional ULF waves. All the momentum diffusion coefficients and time are normalized by $m_e^2 c^2 \Omega_e$ and $2\pi/\Omega_e$, respectively.

3. Numerical Results

[17] At the geosynchronous altitude, the equatorial ambient magnetic field B_0 is about 110 nT, electron cyclotron frequency $f_{ce} = \Omega_e/2\pi = 3.1$ kHz, and proton cyclotron frequency $f_{cp} = \Omega_p/2\pi = 0.167$ kHz. Average electron density n_e increases an order of magnitude from nightside to the dayside: $n_e = 0.6 \sim 30$ cm^{-3} during quite time and $0.4 \sim 10$ cm^{-3} during geomagnetospheric active times at $L = 6.6$ [*Laakso et al.*, 2002], so it is possible that the average electron density may exceed 1 cm^{-3} during active times (e.g., after substorm injection electrons). In the following numerical calculation, we adopt three electron densities $n_e = 2$, 5, 10 cm^{-3},corresponding to $f_{pe}/f_{ce} = 4.1$, 6.5, 9.2, respectively.

[18] The typical parameters of whistler-mode turbulence: $\omega_{lc} = 0.1$, $\omega_{uc} = 0.75$, $\omega_m = 0.35$, $\delta\omega = 0.15$, $A \approx 7.5 R_W (erf(1.7) + erf(2.7))^{-1}$, $R_W = 1.0 \times 10^{-8}$, 4.0×10^{-8}, 9.0×10^{-8}, when $\Delta B_W = 11$, 22, 33 pT [*Parrot and Gaye*, 1994; *Lauben et al.*, 1998; *Baker et al.*, 1998; *Summers et al.*, 2004; *Meredith et al.*, 2001; *Miyoshi et al.*, 2003; *Horne et al.*, 2003]. For the compressional ULF turbulence [*Higuchi and Kokubun*, 1988; *Anderson et al.*, 1990; *Zhu and Kivelson*, 1991; *Baker et al.*, 1998; *Laakso et al.*, 1998; *Rostoker et al.*, 1998; *Mathie et al.*, 2000; *Prikry et al.*, 1998; *Summers and Ma*, 2000b], the frequency range is about 2 mHz $\le f \le$ 15 mHz and the corresponding the minimum wave number $k_{\min}$ is 2.56×10^{-4}. Since only electrons with a velocity larger than the Alfvén speed can be accelerated by compressional ULF turbulence, the momenta of resonant electrons should be larger than 0.0245. $R_U = 1.0 \times 10^{-2}$, 4.0×10^{-2}, 9.0×10^{-2}, when $\Delta B_U = 11$, 22, 33 nT.

[19] In addition, the initial thermal energy of background electrons near the Earth's synchronous orbit is about 10 keV [*Hastings and Garrett*, 1996], and thus $\Delta_b = 0.2$. In general, substorm injection electrons have energies of ~30–300 keV and the electrons with lower energies have a larger flux [*Cayton et al.*, 1989; *Reeves et al.*, 1990; *Friedel et al.*, 1996]. However, since electrons with energies below 100 keV can be scattered into the loss cone, contributing to wave growth, while loss at higher energies is much weaker [*Horne et al.*, 2003a, 2003b], the flux peak of trapped substorm injection electrons are possible at about 100 keV and their temperature $T_s \sim 25$ keV [*Cayton et al.*, 1989], their phase space density $f(p)$ are also the maximum at $E \sim 100$ keV, so we can get $p_0 = 0.66$, $\Delta_s = 0.32$.

3.1. Combined Acceleration by Whistler-Mode and Compressional ULF Turbulences

[20] Electrons can interact with whistler-mode and compressional ULF waves at the same time when both exist together. Furthermore, the efficiency of combined acceleration by whistler-mode and compressional ULF turbulences is different from that of the simple superposition of two efficiencies. Figures 1a, 1b, 1c, and 1d show the momentum distribution functions of electrons that interact with whistler-mode and compressional ULF waves for different time in the case of $\varepsilon = 0.5$, $f_{pe}/f_{ce} = 4.1$. The solid line represents the initial electron momentum distribution function; the others represent $f(p)$ at different time. It is very evident that the number of electrons in the high-energy tail increases with time (see Figure 1a), the peak of substorm injection electrons gradually disappears, and the distribution function becomes flattened. These changes of the electron momentum distribution functions indicate that the initial electrons composed by substorm injection electrons and background electron are accelerated by turbulences after they resonate with turbulences.

[21] It can be seen from Figures 1b and 1c that the larger the amplitude of whistler-mode or compressional ULF turbulence, the more the high-energy electrons. This result is reasonable since turbulences with larger amplitude can offer more energy to accelerate electrons. In addition, the spectrum index of compressional ULF turbulence also has an important influence on the electron acceleration (see Figure 1d), and the smaller the spectrum index is, the greater the number of accelerated electrons is. Therefore the increase of the relativistic electron number is closely related to the intensity of waves after electrons are injected by substorms.

[22] Of course, the combined electron accelerations by whistler-mode and compressional ULF also depend upon the density of electrons. Figure 2 shows that the larger the ratio of the f_{pe}/f_{ce}, the slower the spread of $f(p)$ toward the higher-energy tail, which is in agreement with the results of *Horne et al.* [2003]. This phenomenon is due to the fact that the electron acceleration by whistler-mode waves is affected directly by fluctuation of the electron density during disturbed times. The larger the electron density is, the bigger the ratio of the f_{pe}/f_{ce} is and the lower the efficiency of electron acceleration is. Since the electron acceleration by whistler-mode waves is important in low-density region outside the plasmapause [*Horne et al.*, 2003] for the ratio f_{pe}/f_{ce} is lower in there, electron combined acceleration by

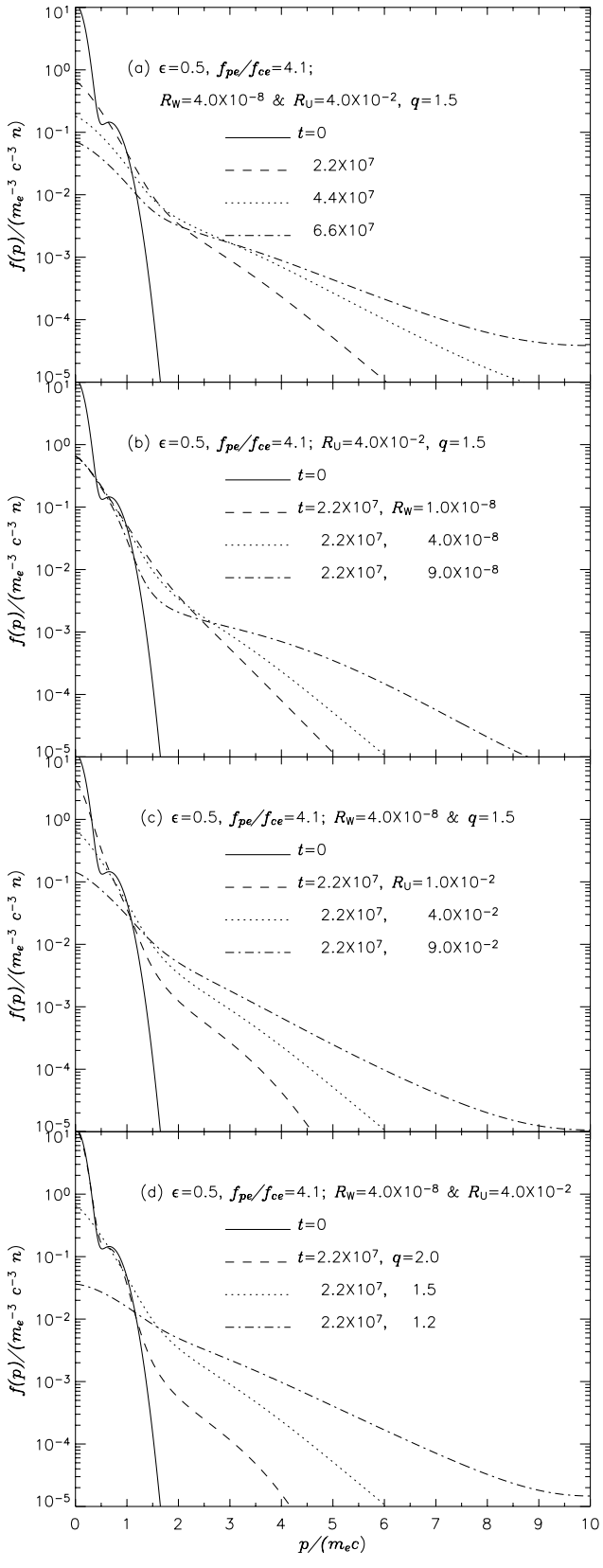

Figure 1. Electron momentum distribution functions at different time for the combined acceleration by whistler-mode and compressional ULF turbulences.

the above two turbulences is more effective in the low-density regions too.

3.2. Difference of Electron Acceleration by Different Wave Turbulences

[23] The combined acceleration by whistler-mode waves and compressional ULF turbulences is most possible since many different mode waves may exist together in the outer radiation belt during the storms/substorms. However, it is also possible that sometimes only one kind of turbulence interacts with electrons by wave-particle resonance, since only one kind of wave exists during some storms/substorms [*O'Brien et al.*, 2003]. Furthermore, some mode waves may be ignored in some regions if these waves are very weak there. Even for a shell with a same L value, the intensities of the whistler-mode and compressional ULF waves may be different at different MLTs. Thus if we neglect compressional ULF waves (or whistler-mode waves), the momentum diffusion coefficient $D(p) = D_W(p)$ (or $D(p) = D_U(p)$). Figure 3 shows the difference of electron accelerations in different cases. The dashed line denotes the electron momentum distribution functions when electrons are accelerated only by whistler-mode waves with $R_W = 4.0 \times 10^{-8}$ for $t = 6.6 \times 10^7$ (i.e., 6 hours). The dotted line denotes the $f(p)$ when electrons are accelerated only by compressional ULF waves with $R_U = 4.0 \times 10^{-2}$, $q = 1.5$. The dash-dotted line denotes the $f(p)$ when electrons are accelerated jointly by two waves.

[24] It can be seen from Figure 3 that only electrons with $p > 0.86$ can be accelerated by whistler-mode waves and the accelerated electrons are mainly substorm injection electrons. This means that substorm injection electrons can be regarded as seed electrons that can be accelerated by whistler-mode turbulence. Different from the whistler-mode turbulence, the compressional ULF waves can accelerate both substorm injection electrons and background hot electrons. In addition, the $f(p)$ spreads toward the high-energy tail more quickly when electrons are accelerated by compressional ULF waves than by whistler-mode waves. The $f(p)$ spreads most quickly in the case of combined acceleration of two turbulences.

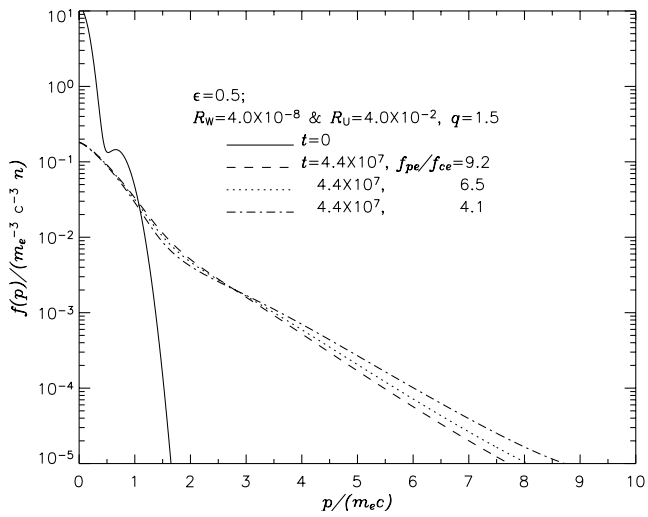

Figure 2. Electron momentum distribution functions at $t = 4.4 \times 10^7$ (i.e., 4 hours) for the different f_{pe}/f_{ce}.

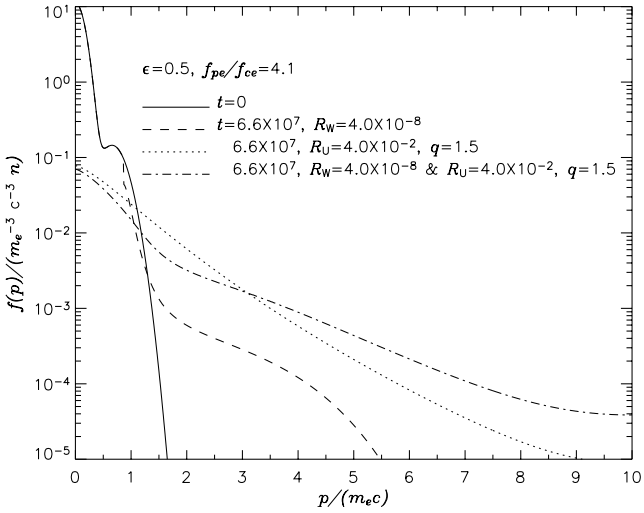

Figure 3. Electron momentum distribution functions at $t = 6.6 \times 10^7$ (i.e., 6 hours) for the different accelerations by whistler-mode, compressional ULF, and combined turbulences, respectively.

[25] In order to estimate the acceleration capability, we define a relativistic electron density ratio $\eta(t)$ which is equal to the ratio of the number of electrons with energy $\geq$1 MeV (i.e., $p \geq 2.78$) to the total number of electrons. Figure 4 shows the temporal evolution of the relativistic electron density ratio $\eta(t)$ for three cases: whistler-mode turbulence, compressional ULF turbulence, and the combined turbulence. The relevant parameters are the same with those in Figure 3. At $t = 8.8 \times 10^7$ (i.e., 8 hours), the relativistic electron density ratio $\eta(t)$ is 0.0799 for the whistler-mode turbulence, $\eta(t)$ is 0.615 for the compressional ULF turbulence, and $\eta(t)$ is 0.925 for the combined turbulences. Apparently, the combined acceleration cannot be regarded as a simple superposition of the accelerations generated separately by the two kinds of turbulences. The acceleration efficiency of the compressional ULF turbulence is larger than that of the whistler-mode turbulence. The efficiency of combined acceleration of the whistler-mode and the compressional ULF turbulences is largest. This result is in agreement with the statistical observational results of *O'Brien et al.* [2003]. The combined acceleration of the whistler-mode and compressional ULF turbulences can cause the number density of the relativistic electrons increase largely within about 8 hours. Therefore it is very possible that the relativistic electrons enhancement on 10 January 1997 is the result of the combined acceleration by different waves.

[26] Finally, we can draw two conclusions from Figures 3 and 4. (1) Even in the magnetospheric quiet time (i.e., absence of substorm injection electrons), as long as the solar wind disturbance can excite ULF turbulences in the magnetosphere, a relativistic electron flux enhancement event can occur in the radiation belt. (2) Larger flux enhancement events of relativistic electrons always occur in the active time of the magnetosphere, since a substorm can offer more seed electrons and the strong turbulences that can accelerate these electrons. Substorm injection electrons may be a main source of relativistic electrons near the geosynchronous orbit during the magnetic storms, especially during those storms that are accompanied by a series of substorms.

4. Conclusions and Discussion

[27] In this paper, in the quasi-linear approximation, we study the electron acceleration due to whistler-mode and compressional ULF wave turbulences near the geosynchronous orbit. On the basis of the observation data, we chose the spectrum parameters. The main results are summarized as follows:

[28] 1. The combined acceleration by two turbulences is the more effective at the low-density region outside the plasmapause, since the ratio f_{pe}/f_{ce} is lower there. The larger the amplitude of turbulence, the greater the number of accelerated electrons. Near the geosynchronous orbit, the combined acceleration by the whistler-mode and the compressional ULF turbulences can cause the number density of the relativistic electrons to increase largely within about 8 hours.

[29] 2. The whistler-mode turbulence can only accelerate substorm injection electrons with several hundreds of keV. So the whistler-mode turbulence acceleration may only play a role during substorms. However, the compressional ULF turbulence can accelerate both lower-energy background electrons and substorm injection electrons. So the compressional ULF turbulence may accelerate electrons during both substorms and quiet times.

[30] 3. Near the geosynchronous orbit, the compressional ULF turbulence can accelerate electrons more effectively than the whistler-mode turbulence, and it can accelerate more electrons to a higher energy than the whistler-mode turbulence. The combined acceleration of electrons by whistler-mode and compressional ULF turbulences is most effective.

[31] 4. Since during the magnetospheric active time a substorm can offer hot seed electrons and stronger turbulences, large flux enhancement events of relativistic electrons always occur during the active times of the magnetosphere. During some magnetic storms that are

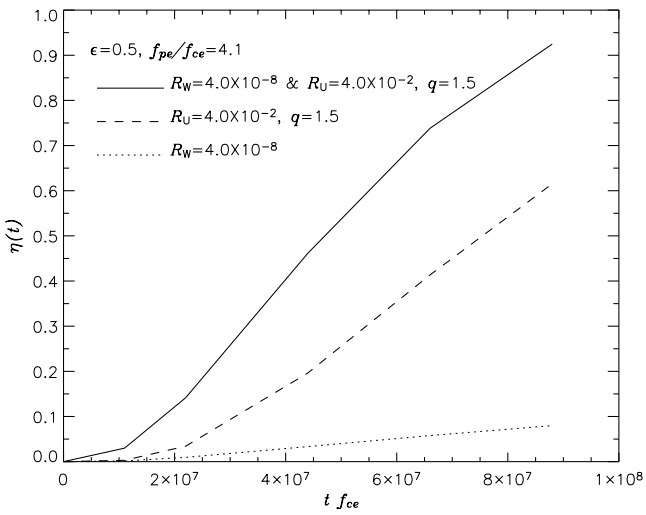

Figure 4. Temporal evolution of $\eta(t)$ with time for the different accelerations by whistler-mode, compressional ULF, and combined turbulences, respectively.

composed of a series of substorms, extremely large flux enhancement events of relativistic electrons can also occur.

[32] Here we only study wave-electron interactions on the basis of the observation data near geosynchronous orbit and draw the conclusion that the electron acceleration by the compressional ULF turbulence is more effective than the whistler-mode turbulence. In other space regions, the amplitudes of compressional ULF and whistler-mode turbulences may be different and hence the conclusion may be different. Moreover, the new injection sources and loss of electrons may affect the number density increase of relativistic electrons. We will take into consideration these factors in the future work.

[33] **Acknowledgments.** This work was supported by NSFC 40025413. The authors are grateful to X. Li for many useful discussions and suggestions.

[34] Lou-Chuang Lee thanks Richard Horne and Richard Selesnick for their assistance in evaluating this paper.

References

Anderson, B. J., M. J. Engebretson, S. P. Rounds, L. J. Zanetti, and T. A. Potemra (1990), A statistical study of Pc3-5 pulsations observed by the AMPTE/CCE magnetic fields experiment: 1. Occurrence distributions, *J. Geophys. Res.*, *95*, 10,495.

Baker, D. N., T. I. Pulkkinen, X. Li, S. G. Kanekal, J. B. Blake, R. S. Selesnick, M. G. Henderson, G. D. Reeves, H. E. Spence, and G. Rostoker (1998), Coronal mass ejections, magnetic clouds, and relativistic magnetospheric electron events: ISTP, *J. Geophys. Res.*, *103*, 17,279.

Blake, J. B., D. N. Baker, N. Turner, K. W. Ogilvie, and R. P. Lepling (1997), Correlation of changes in the outer-zone relativistic-electron population with upstream solar wind and magnetic field measurements, *Geophys. Res. Lett.*, *24*, 927.

Cao, J.-B., G.-C. Zhou, X.-Y. Wang, D.-J. Wang, and C.-L. Cai (2002), Relationship among the electron event in April–May 1998, the magnetic storm and interplanetary condition, paper presented at 2002 Western Pacific Geophysics Meeting, AGU, Wellington, New Zealand.

Cayton, T. E., R. D. Belian, S. P. Gary, T. A. Fritz, and D. N. Baker (1989), Energetic electron components at geosynchronous orbit, *Geophys. Res. Lett.*, *16*, 147.

Elkington, S. R., M. K. Hudson, and A. A. Chan (1999), Acceleration of relativistic electrons via drift-resonance interaction with toroidal-mode Pc5 ULF oscillations, *Geophys. Res. Lett.*, *26*, 3273.

Friedel, R. H. W., A. Korth, and G. Kremser (1996), Substorm onsets observed by CREES: Determination of energetic particle source regions, *J. Geophys. Res.*, *101*, 13,137.

Hastings, D., and H. Garrett (1996), *Spacecraft-Environment Interactions*, Cambridge Univ. Press, New York.

Higuchi, T., and S. Kokubun (1988), Waveform and polarization of compressional Pc5 waves at geosynchronous orbit, *J. Geophys. Res.*, *93*, 14,433.

Horne, R. B., S. A. Glauert, and R. M. Thorne (2003), Resonant diffusion of radiation belt electrons by whistler chorus, *Geophys. Res. Lett.*, *30*(10), 1493, doi:10.1029/2003GL016963.

Hudson, M. K., S. R. Elkington, J. G. Lyon, and C. C. Goodrich (2000), Increase in relativistic electron flux in the inner magnetosphere: ULF wave mode structure, *Adv. Space Res.*, *25*, 2327.

Hudson, M. K., S. R. Elkington, J. G. Lyon, M. J. Wiltberger, and M. Lessard (2001), Radiation belt electron acceleration by ULF wave drift resonance: Simulation of 1997 and 1998 storms, in *Space Weather*, *Geophys. Monogr. Ser.*, vol. 125, edited by P. Song, p. 289, AGU, Washington, D. C.

Iles, R. H. A., A. N. Fazakerley, A. D. Johnstone, N. P. Meredith, and P. Buhler (2002), The relativistic electron response in the outer radiation belt during magnetic storms, *Ann. Geophys.*, *20*, 957.

Laakso, H., et al. (1998), Field-line resonances triggered by a northward IMF turning, *Geophys. Res. Lett.*, *25*, 2991.

Laakso, H., R. Pfaff, and P. Janhunen (2002), Polar observeration of electron density distribution in the Earth's magnetosphere. 1. Statistical results, *Ann. Geophys.*, *20*, 1711.

Lauben, D. S., U. S. Inan, T. F. Bell, D. L. Kirchner, G. B. Hospodarsky, and J. S. Pickett (1998), VLF chorus emissions obsvered by PLOAR during the January 10, 1997, magnetic cloud, *Geophys. Res. Lett.*, *25*, 2995.

Li, L.-Y., J.-B. Cao, and G.-C. Zhou (2004), Acceleration of "seed electrons" by whistler turbulence near the geosynchronous orbit, *Chin. J. Geophys.*, *47*, 756.

Li, X., D. N. Baker, M. Temerin, T. E. Cayton, E. G. D. Reeves, R. S. Selesnick, J. B. Blake, G. Lu, S. G. Kanekal, and H. Singer (1999), Rapid enhancements of relativistic electrons deep in the magnetosphere during May 15, 1997 magnetic, *J. Geophys. Res.*, *104*, 4467.

Mathie, R. A., and I. R. Mann (2000), Observations of Pc5 field line resonance azimuthal phase speeds: A diagnostic of their excitation mechanism, *J. Geophys. Res.*, *105*, 10,713.

Meredith, N. P., R. B. Horne, and R. R. Anderson (2001), Substorm dependence of chorus amplitudes: Implications for the acceleration of electrons to relativistic energies, *J. Geophys. Res.*, *106*, 13,165.

Meredith, N. P., R. B. Horne, R. H. A. Illes, R. M. Thorne, D. Heynderickx, and R. R. Anderson (2002), Outer zone relativistic electron acceleration associated with substorm-enhanced whistler mode chorus, *J. Geophys. Res.*, *107*(A7), 1144, doi:10.1029/2001JA900146.

Meredith, N. P., M. Cain, R. B. Horne, R. M. Thorne, D. Summers, and R. R. Anderson (2003), Evidence for chorus-driven electron acceleration to relativistic energies from a survey of geomagnetically disturbed periods, *J. Geophys. Res.*, *108*(A6), 1248, doi:10.1029/2002JA009764.

Miyoshi, Y., A. Morioka, T. Obara, H. Misawa, T. Nagai, and Y. Kasahara (2003), Rebuilding process of the outer radiation belt during the 3 November 1993 magnetic storm: NOAA and Exos-D observations, *J. Geophys. Res.*, *108*(A1), 1004, doi:10.1029/2001JA007542.

Nakamura, R., J. B. Blake, S. R. Elkington, D. N. Baker, W. Baumjohann, and B. Klecker (2002), Relationship between ULF waves and radiation belt electrons during the March 10, 1998, storm, *Adv. Space Res.*, *30*, 2163.

O'Brien, T. P., K. R. Lorentzen, I. R. Mann, N. P. Meredith, J. B. Blake, J. F. Fennell, M. D. Looper, D. K. Milling, and R. R. Anderson (2003), Energization of relativistic electrons in the presence of ULF power and MeV microbursts: Evidence for dual ULF and VLF acceleration, *J. Geophys. Res.*, *108*(A1), 1004, doi:10.1029/2001JA007542.

Parrot, M., and C. A. Gaye (1994), A statistical survey of ELF waves in a geostationary orbit, *Geophys. Res. Lett.*, *21*, 2463.

Posch, J. L., M. J. Engebretson, V. A. Pilipenko, W. J. Hughes, C. T. Russell, and L. J. Lanzerotti 2003, Characterizing the long-period ULF response to magnetic storms, *J. Geophys. Res.*, *108*(A1), 1029, doi:10.1029/2002JA009386.

Prikry, P., R. A. Greenwald, G. J. Sofko, J. P. Villian, C. W. S. Ziesolleck, and E. Friis-Christensen (1998), Solar-wind-driven pulsed magnetic reconnection at the dayside magnetopause, Pc5 compressional oscillations, and field line resonances, *J. Geophys. Res.*, *103*, 17,307.

Reeves, G. D. (1998), Relativistic electrons and magnetic storms: 1992–1995, *Geophys. Res. Lett.*, *25*, 1817.

Reeves, G. D., T. A. Fritz, T. E. Cayton, and R. D. Belian (1990), Multi-satellite measurements of the substorm injection system, *Geophys. Res. Lett.*, *17*, 2015.

Reeves, G. D., K. L. McAdams, R. H. W. Friedel, and T. P. O'Brien (2003), Acceleration and loss of relativistic electrons during geomagnetic storms, *Geophys. Res. Lett.*, *30*(10), 1529, doi:10.1029/2002GL016513.

Rostoker, G., S. Skone, and D. N. Baker (1998), On the origin of relativistic electrons in the magnetosphere associated with some geomagnetic storms, *Geophys. Res. Lett.*, *25*, 3701.

Russell, C. T. (2000), How northward turnings of the IMF can lead to substorm expansion onsets, *Geophys. Res. Lett.*, *27*, 3257.

Schlickeiser, R., and J. A. Miller (1998), Quasi-linear theory of cosmic ray transport and acceleration: The role of oblique magnetohydrodynamic waves and transit-time damping, *Astrophys. J.*, *492*, 352.

Selesnick, R. S., and J. B. Blake (1998), Radiation belt electron observations following the January 1997 magnetic cloud event, *Geophys. Res. Lett.*, *25*, 2553.

Steinacker, J., and J. A. Miller (1992), Stochastic gyroresonant electron acceleration in a low-beta plasma interaction with parallel transverse cold plasma waves, *Astrophys. J.*, *393*, 764.

Summers, D., and C. Y. Ma (2000a), A model for generating relativistic electrons in the Earth's inner magnetospheres based on gyroresonant wave-particle interactions, *J. Geophys. Res.*, *105*, 2625.

Summers, D., and C. Y. Ma (2000b), Rapid acceleration of electrons in the magnetosphere by fast-mode MHD waves, *J. Geophys. Res.*, *105*, 15,887.

Summers, D., C. Y. Ma, N. P. Meredith, R. B. Horne, R. M. Thorne, and R. R. Anderson (2004), Modeling outer-zone relativistic electron response to whistler-mode chorus activity during substorms, *J. Atmos. Sol. Terr. Phys.*, 66,133.

Tsurutani, T. B., and E. J. Smith (1977), Two types of magnetospheric ELF chorus and their substorm dependencies, *J. Geophys. Res.*, *82*, 5112.

Wrenn, G. L., and R. J. K. Smith (1996), The ESD threat to GEO satellites: Empirical models for observed effects due to both surface and internal charging, in *ESA Symposium Proceedings on Environment Modelling for Space-Based Applications*, *SP-392*, p. 121, Eur. Space Res. and Tech. Cent., Noorwijk, Netherlands.

Zhou, G. C., X. Y. Wang, D. J. Wang, J. B. Cao, and C. L. Cai (2001), MeV electron-flux enhancement events at the geosynchronous orbit in April–May 1998, *Chin. J. Geophys.*, *44*, 285.

Zhu, X., and M. G. Kivelson (1991), Compressional ULF waves in the outer magnetosphere: 1. Statistical study, *J. Geophys. Res.*, *96*, 19,451.

J. Cao, L. Li, and G. Zhou, Center for Space Science and Applied Research, Chinese Academy of Sciences, Beijing 100080, China. (lyli@center.cssar.ac.cn)